North Atlantic Evidence for a Unipolar Icehouse Climate State at the Eocene-Oligocene Transition

James F. Spray[1] [ID], Steven M. Bohaty[1] [ID], Andrew Davies[2] [ID], Ian Bailey[3] [ID], Brian W. Romans[4], Matthew J. Cooper[1] [ID], James A. Milton[1], and Paul A. Wilson[1] [ID]

[1]National Oceanography Centre Southampton, University of Southampton, Waterfront Campus, Southampton, UK, [2]Halliburton, Abingdon, UK, [3]Camborne School of Mines and Environment and Sustainability Institute, College of Engineering, Mathematics and Physical Sciences, University of Exeter, Penryn Campus, Penryn, UK, [4]Department of Geosciences, Virginia Tech, Blacksburg, VA, USA

Abstract Earth's climate transitioned from a warm unglaciated state to a colder glaciated "icehouse" state during the Cenozoic. Extensive ice sheets were first sustained on Antarctica at the Eocene-Oligocene Transition (EOT, ~34 Ma), but there is intense debate over whether Northern Hemisphere ice sheets developed simultaneously at this time or tens of millions of years later. Here we report on EOT-age sediments that contain detrital sand from Integrated Ocean Drilling Program Sites U1406 and U1411 on the Newfoundland margin. These sites are ideally located to test competing hypotheses of the extent of Arctic glaciation, being situated in the North Atlantic's "iceberg alley" where icebergs, calved from both the Greenland Ice Sheet today, and the Laurentide Ice Sheet during the Pleistocene, are concentrated by the Labrador Current and deposit continentally derived detritus. Here we show that detrital sand grains present in these EOT-aged sediments from the Newfoundland margin, initially interpreted to represent ice rafting, were sourced from the midlatitudes of North America. We find that these grains were transported to the western North Atlantic by fluvial and downslope processes, not icebergs, and were subsequently reworked and deposited by deep-water contour currents on the Newfoundland margin. Our findings are inconsistent with the presence of extensive ice sheets on southern and western Greenland and the northeastern Canadian Arctic. This contradicts extensive bipolar glaciation at the EOT. The unipolar icehouse arose because of contrasting latitudinal continental configurations at the poles, requiring more intense Cenozoic climatic deterioration to trigger extensive Northern Hemisphere glaciation.

1. Introduction

It is widely inferred that continental-scale ice sheets first developed on Antarctica across the Eocene-Oligocene Transition (EOT; Hambrey & Barrett, 1993; Kennett, 1977; Miller et al., 1991; Zachos et al., 1996). While the Arctic likely supported sea ice and coastal outlet glaciers prior to this time (Davies et al., 2009; Moran et al., 2006; St. John, 2008), intense debate exists over whether the northern continents were extensively glaciated at the same time as Antarctica during the Paleogene. The traditionally accepted view is that Greenland has experienced multiple glaciations since the late Miocene (~7 Ma; Larsen et al., 1994) with more extensive glaciation of the Northern Hemisphere in the late Pliocene (~2.7 Ma; Bailey et al., 2013). Debate centers around two main lines of evidence: (i) excursions in Paleogene (~66–23 Ma) benthic foraminiferal oxygen isotope records that are too large to be accommodated by Antarctic ice growth alone (Coxall et al., 2005; Tripati et al., 2005) and (ii) ice-rafted debris (IRD) in strata of middle Eocene-to-early Oligocene age (39-30 Ma) from the Norwegian-Greenland Sea (NGS; Figure 1; Eldrett et al., 2007; Tripati et al., 2008). One interpretation is that these records together indicate simultaneous bipolar Paleogene glaciation, with ice sheets on multiple Northern Hemisphere continents (Dawber & Tripati, 2011; Tripati et al., 2005; Tripati et al., 2008)—or at least Greenland (Tripati & Darby, 2018). Another interpretation is that significant Northern Hemisphere glaciation did not occur at the EOT because the northern continents were too warm in summer to support major ice sheets (DeConto et al., 2008; Eldrett et al., 2009; Solgaard et al., 2013). In this second interpretation, the oxygen isotope-derived ice budgets presented in favor of bipolar glaciation are overestimates because they are based on inadequate records and/or incorrect accounting for ocean cooling (Coxall et al., 2005; Edgar et al., 2007; Lear et al., 2008), and IRD deposited in the NGS is explained by small outlet glaciers on East Greenland, and potentially also by Arctic Ocean sea ice (Eldrett et al., 2007; Moran et al., 2006; St. John, 2008).
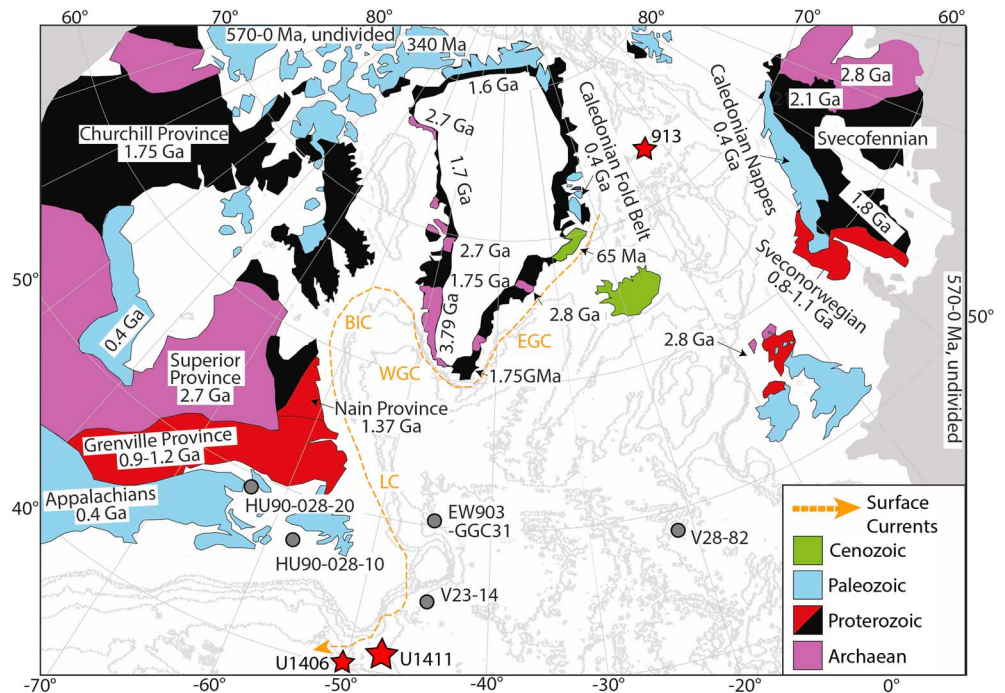
Figure 1. Circum-North Atlantic Ocean, showing our Integrated Ocean Drilling Program study sites (U1406 and U1411) and other sites relevant to our study, modern-day surface currents responsible for transporting icebergs, and the terranes of the North Atlantic margins. ECG = East Greenland Current, WGC = West Greenland Current, BIC = Baffin Island Current, and LC = Labrador Current. Modified from Bailey et al. (2012).

In a recent study of detrital grains deposited at Ocean Drilling Program Site 913 in the NGS, a dynamic cryosphere with episodic growth of continental ice in the Northern Hemisphere is interpreted to have initiated from the middle Eocene (~44 Ma; Tripati & Darby, 2018; Figure 1). An ancient ice cap covering at least a large portion of East Greenland is invoked, together with possible ice-rafting sources around the rim of the Arctic Ocean. Based on these results, Tripati and Darby (2018) question the time-sequential CO_2-temperature threshold model for the onset of bipolar glaciation developed by DeConto et al. (2008). That model suggests that the CO_2 level at which ice sheet (as opposed to ice-cap or glacier) inception is triggered is lower for the Northern Hemisphere than the Southern Hemisphere, and therefore, the circum-Arctic continents are less prone to pre-Neogene glaciation than Antarctica. By questioning the sequential CO_2 threshold model for bipolar glaciation based on their provenance study of detrital grains at Site 913 (NGS; Figure 1), Tripati and Darby (2018) invoke extensive Paleogene bipolar glaciation. However, evidence for ice extent more substantial than upland coastal outlet glaciers or a small ice cap on East Greenland is needed to substantiate this argument.

Deep-sea sediments from the northwestern Atlantic Ocean may hold further clues to the nature of Paleogene glaciation in Greenland and northeastern Canada. Detrital sands and coarse silts and conspicuous 1- to 5-mm grain aggregates were recently reported in sediments of EOT age from Integrated Ocean Drilling Program (IODP) Expedition (Exp.) 342 Sites U1406 and U1411 (Figure 1) and were proposed to be of ice-rafted origin (Norris et al., 2014). These sites lie within the North Atlantic Ocean's modern day "iceberg alley," where icebergs calved from northeastern Canada and the southern and western margins of the Greenland Ice Sheet (Bigg et al., 2014), and not eastern Greenland, are concentrated by the Labrador Current and deposit IRD (Bigg et al., 1996). An improved understanding of the origin of these detrital grains therefore offers a way to shed new light on the plausibility of the suggestion that the Northern Hemisphere became extensively glaciated at the EOT (Tripati et al., 2005; Tripati & Darby, 2018), as evidence for iceberg-rafting sources from more locations than just eastern Greenland at this time is required to substantiate this claim.

Here we report the results of a sedimentary and geochemical study of detrital grains in sediments of EOT age from IODP Sites U1406 andU1411. We compare these detrital grains to (i) the overlying Pleistocene

sequence at Site U1411 and (ii) the EOT sequence from the NGS (Site 913; Figure 1). In doing so, we test the hypothesis that the EOT-age detrital sands at Sites U1406 and U1411 are ice-rafted in origin and derived from a large ice sheet on Greenland, with iceberg calving sources on its southern and western margins (as today), and perhaps from elsewhere, especially in northeastern Canada. Our results directly address the controversy over whether the Northern and Southern Hemispheres share one broadly similar CO_2-temperature threshold for glaciation (Tripati et al., 2005; Tripati & Darby, 2018) or whether two climate thresholds were crossed during the Cenozoic to establish our modern bipolar icehouse state (DeConto et al., 2008).

2. Materials and Methods

2.1. Study Sites

Widespread evidence exists for extensive ice-rafting across the open North Atlantic Ocean during Plio-Pleistocene glaciations (Bailey et al., 2013; Bolton et al., 2018; Raymo et al., 1989; Shackleton et al., 1984), but our ability to test for ice-rafting during older intervals, such as the EOT, has been hampered by major gaps in the deep-sea geological record because of hiatuses and condensed horizons attributed to deep-ocean current activity (Miller & Tucholke, 1983). Recently, however, an expanded (sedimentation rates up to ~3 cm/kyr) and shallowly buried (125–195 m below seafloor) sequence of EOT sediments (~32.8–35.2 Ma) was recovered (Norris et al., 2014) at IODP Site U1411, drilled into a perched contourite sediment drift (Boyle et al., 2017) deposited in the Northwest Atlantic Ocean on the Southeast Newfoundland Ridge (SENR; 41°37.1′N, 49°00′W; ~3,300-m water depth; Figure 1). A second, less expanded (sedimentation rates up to ~1 cm/kyr), sequence of EOT-age sediments was also recovered at IODP Site U1406 (40°20.99′N, 51°38.99′W; ~3,800-m water depth; Figure 1) on the adjacent J-Anomaly Ridge (JAR; Norris et al., 2014), positioned ~250 km to the southwest of Site U1411.

During shipboard analysis of the Site U1406 and U1411 sediments, fine detrital sands and coarse silts of EOT-age were observed (Norris et al., 2014). In addition to being disseminated through the largely homogenized nannofossil ooze (Site U1406) and silty clay (Site U1411) sediments that constitute the EOT intervals at these sites, loosely aggregated 1- to 5-mm scale pockets of the same detrital sand and silt were also observed on core surfaces. These clasts were tentatively determined during IODP Exp. 342 to be siltstone dropstones (Norris et al., 2014) rafted by icebergs to the SENR and JAR. Both the SENR and JAR are bathymetric highs isolated from the influence of downslope sedimentary processes originating from the Newfoundland continental margin (Boyle et al., 2017).

2.2. Detrital Grain Concentration

To determine temporal changes in the concentration of the detrital sand grains across the EOT at our two study sites, we calculated the abundance of detrital sand grains in the Site U1411 and Site U1406 late Eocene-Oligocene intervals by counting the number of sand grains in each sample and dividing by the dry bulk weight. Laser grain size analysis of several samples from the Site U1411 Paleogene interval (Figure S1 in the supporting information) revealed that the vast majority of the sand was fine- to medium-grained, and so focused the grain counts on the 63- to 500-μm fraction. The >500-μm fraction for each sample was also examined for any coarse-grained sand. Counts were also performed in the same way on samples from the Site U1411 Pleistocene interval for comparison. Mica, which was present in the samples, was not counted because sieving does not provide an accurate reflection of its grain size due to its platey nature. Mica also has a relatively low settling velocity and can therefore be carried significant distances by ocean currents (Garzanti et al., 2008).

2.3. Grain Surface Textural Analysis

To test for ice rafting activity during the EOT, we examined the texture of the detrital quartz sands at Sites U1406 and U1411, and also at Site 913 for comparison (Figure 1), to explore the transport history of these grains. We analyzed only quartz grains >200 μm, because there are differences in the expression of surface textures below this threshold (Krinsley & Doornkamp, 2011). Over 600 samples from the EOT sequence at U1411 were sieved at >200 μm and examined for quartz grains using a binocular microscope. The majority of the samples examined did not contain quartz grains in the >200-μm size fraction, but 48 samples contained 1-5 grains. From these 48 samples, a total of 111 suitable quartz grains were picked for analysis (Data Set S1 in the supporting information). These samples were compared to representative samples

from the sand- and dropstone-rich overlying Pleistocene sequence at Site U1411 and the Eocene-to-Oligocene sequence from Site 913. Five samples were analyzed from the Site U1411 Pleistocene sequence, and six samples were analyzed from the Site 913 EOT interval; quartz grains >200 μm in these samples were abundant, allowing ~20-30 grains to be easily picked from each sample. In total, 101 grains were analyzed from the Site U1411 Pleistocene interval, and 185 grains were analyzed from the Site 913 EOT interval (Data Set S1).

For textural analysis, the grains from each interval were mounted onto aluminum stubs and sputter coated in gold film in preparation for scanning electron microscopy (SEM) analysis using a Leo 1450VP SEM with an attached light element PGT energy-dispersive spectrometer at the University of Southampton- National Oceanography Centre, Southampton (NOCS). The surface textures, roundness, and relief were assessed for each grain analyzed (Table S1 in the supporting information). A suite of surface textures were analyzed for each grain, based on a compilation of several studies (Dunhill, 1998; Helland & Holmes, 1997; Mahaney et al., 2001; St. John et al., 2015; Williams & Morgan, 1993). Each texture was classed as being either mechanical or chemical in its weathering origin in these studies; mechanical textures relate to physical damage caused by grains being ground/smashed/split, whereas chemical textures result from dissolution and reprecipitation of silica immersed in water (Krinsley & Doornkamp, 2011). The relative abundance of each texture was calculated on the grains from within each interval. Silica dissolution was graded using the scheme of St. John et al. (2015). Roundness was graded using Power's scale (Powers, 1953), and the relief of each grain was classified as being low, medium, or high. We used Euclidean distances to further explore the differences in the surface textures between each interval (Text S1 in the supporting information).

2.4. Sedimentology

To determine whether the aggregate clasts at Site U1411 represent ice-rafted dropstones, we studied their distribution, morphology, and composition. We compared these clasts to sand-sized detrital material and grain aggregates from the EOT interval at Site 913 that were previously interpreted as dropstones (Eldrett et al., 2007; Tripati et al., 2008). The grain aggregates described during IODP Exp. 342 were examined in core sections from the EOT composite interval at Site U1411 (Sections U1411 B-15H-1 to U1411 B-20H-4 and U1411C-6H-3 to U1411C-12H-6). The size and mineralogy of the component grains of the aggregates were investigated via SEM and energy-dispersive spectrometer to confirm that they resembled the grains disseminated throughout the sediment (Text S1). The three-dimensional structure of the aggregates within the background sediment of the cores was explored using X-ray microcomputed tomography at the μVIS X-Ray Imaging Centre, University of Southampton. These analyses were conducted on a half-core round (~2 cm in thickness) from the aggregate-rich Oligocene-aged interval of Site U1411 (Sample U1411B-7H-6W, 58-60 cm), showing several grain aggregates on its surface. We also inspected the Eocene-Oligocene interval at Site 913 for features similar to the Site U1411 grain aggregates (Sections 913B-23R-1 to 913B-27R-5).

2.5. Geochemical Provenance

We explored the geochemical provenance of the EOT-age detrital grains from Site U1411 to determine whether sand grains in the EOT interval at this site were sourced from possible glacier calving sites (i.e., south and west Greenland, east Greenland, or northeastern Canada). We analyzed the lead (Pb) isotope composition of feldspars and the strontium-neodymium (Sr-Nd) isotope compositions of the sand-sized detrital fraction of grains extracted from samples from the Site U1411 EOT interval. These results were compared to the published isotopic signatures of circum-North Atlantic continental terranes. For Pb, we hand-picked 350-500 sand-sized (>63 μm) feldspar grains from 24 samples from the U1411 EOT interval. Each sample was digested *en masse*, because none of the feldspars found were large enough to be analyzed individually. Pb was separated via column chemistry using AG1x8 anion exchange resin following the methods of Baker et al. (2004). Pb isotopes were analyzed using a multicollector inductively coupled plasma mass spectrometer (Thermo Scientific Neptune) at the University of Southampton, NOCS. For Sr and Nd, we leached and digested the coarse (>63 μm) detrital fractions of eight samples from the U1411 EOT interval, following the methods of Lang et al. (2014). Nd was isolated from each sample using two column passes: first AG50-X8 200-400 mesh cation columns and second LN Spec columns. Nd isotopes were analyzed at NOCS via multicollector inductively coupled plasma mass spectrometer. We isolated Sr for isotopic analysis using columns containing Sr-Spec resin; samples were then loaded onto stubs with a Ta filament, following which

we analyzed Sr isotopes using a Thermofisher Triton multicollector thermal isolation mass spectrometer at the University of Southampton- NOCS (full details of the analytical methods are provided in Text S1).

3. Results

3.1. Detrital Sand Grains Found in Newfoundland Sediments of EOT Age

A long-term increase is observed in the concentrations of detrital sand grains deposited at Sites U1406 and U1411 from the late Eocene through to the Oligocene and in the Pleistocene (Figure 2). Sand grains in the >500-μm-size fraction, which are typically present in IRD, are abundant in sediments of Pleistocene age from Site U1411. In contrast, sand grains >500 μm are absent from the underlying sediments of Paleogene age at the same site (Figure 2). In these older sediments of Site U1411, the detrital sand grains are predominantly very fine (63–125 μm) and well sorted (Figure S1), unlike IRD. The stratigraphic distribution of these finer-grained sands reveals an increase in concentration from <100 grains/g prior to ~35 Ma to ~10,000 grains/g by the Mid-Oligocene Glacial Interval (~28–26 Ma; Liebrand et al., 2017; Figure 2). Grain abundance distribution at Site U1406 shows a similar trend, albeit at lower concentrations (Figure 2).

The surface textures observed on quartz grains from the Site U1411 EOT interval are less angular (Figure 3a) than those from both the Pleistocene sequence at the same site (Figure 3b) and EOT-aged sands from Site 913 (Figure 3c). About 55% of the grains from the Site U1411 EOT interval are subrounded to well rounded, compared to only 25% and 21% for the Site 913 EOT and Site U1411 Pleistocene grains, respectively (Table 1). All chemical surface textures are 15–25% more common on Site U1411 EOT grains than on their Pleistocene counterparts, and ~7–25% more common than on Site 913 grains. Low relief and common-to-pervasive silica dissolution features are far more common in the EOT-aged grains from Site U1411 (42% and 68%, respectively) than either the Site U1411 Pleistocene (14% and 49%) or Site 913 EOT (11% and 54%) grains. Mechanical textures such as impact pits, conchoidal fractures, arc and straight step-like fractures, and gouges/striations are all more common in the Pleistocene-aged grains at Site U1411 and the EOT grains from Site 913 than in the EOT Site U1411 grains (Tab. 1). The Site 913 EOT and Site U1411 Pleistocene intervals are also closer in Euclidean Space (50) than either the EOT pairing from both sites (69) or the EOT and Pleistocene pairing at Site U1411 (85).

At open-ocean subpolar North Atlantic sites, IRD of Plio-Pleistocene age is found in high concentrations in sediments deposited during major Northern Hemisphere glacials (Bailey et al., 2012; Raymo et al., 1989; Shackleton et al., 1984). This IRD is distinguished by poorly sorted detrital grains exhibiting a high degree of angularity and abundant mechanically induced surface textures, when compared to grains transported by fluvio-marine processes (Bailey et al., 2012; Krinsley & Doornkamp, 2011; Mahaney et al., 2001). The sedimentary properties of sand grains in the EOT sequence at Site 913 and the Pleistocene interval at Site U1411 are consistent with this description, indicating an ice-rafted origin. High angularity and high frequencies of mechanical surface textures indicate that these are relatively fresh grains sculpted mechanically (e.g., through glacial crushing) and were transported by icebergs without significant saltation (Mahaney et al., 2001). In contrast, the EOT grains from Site U1411 are more rounded and show low-medium relief and high frequencies of chemical surface textures, implying transport by fluvio-marine processes with extensive saltation and submersion (Krinsley & Doornkamp, 2011; Mahaney et al., 2001), rather than by iceberg rafting. It is also worth noting that dolomitic detrital clasts, which are common in Pleistocene-aged IRD (during ambient ice-rafting episodes) from Hudson Bay sources, are absent in the Site U1411 EOT interval (Andrews & Tedesco, 1992), further contradicting an ice-rafted origin for the EOT-aged sands and silts in favor of fluvio-marine processes. However, this interpretation does not explain the conspicuous grain aggregates (Figure 4a) identified at the Newfoundland margin sites that have been attributed (Norris et al., 2014) to ice rafting.

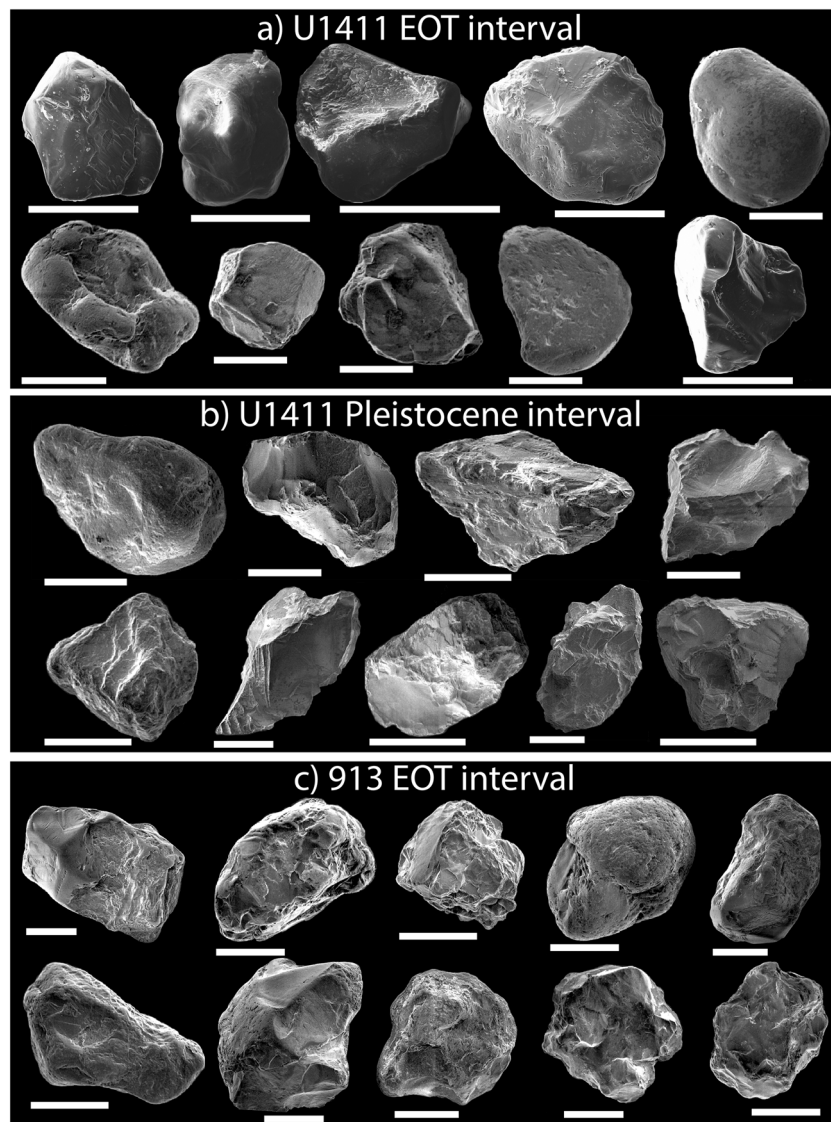### 3.2. Grain Aggregates and Ice Rafting

The grain aggregates are conspicuous on the surfaces of Site U1411 split core because of their lightness in color, which contrasts with their host lithology, a dark green homogenous thoroughly bioturbated silty clay. The aggregates are elliptical to irregular in shape and ~1–10 mm in diameter (Figures 4a and 4c). SEM and elemental analysis reveal that the aggregates are composed predominantly of quartz grains with a minor contribution of feldspars and accessory minerals. These grains predominantly fall within the coarse silt-to-very fine sand size fraction (~31 to 125 μm). In contrast, the EOT interval at Site 913 contains coarser detrital material than Site U1411, with coarse sand and occasional pebbles. Some of these clasts are sedimentary lithic fragments,
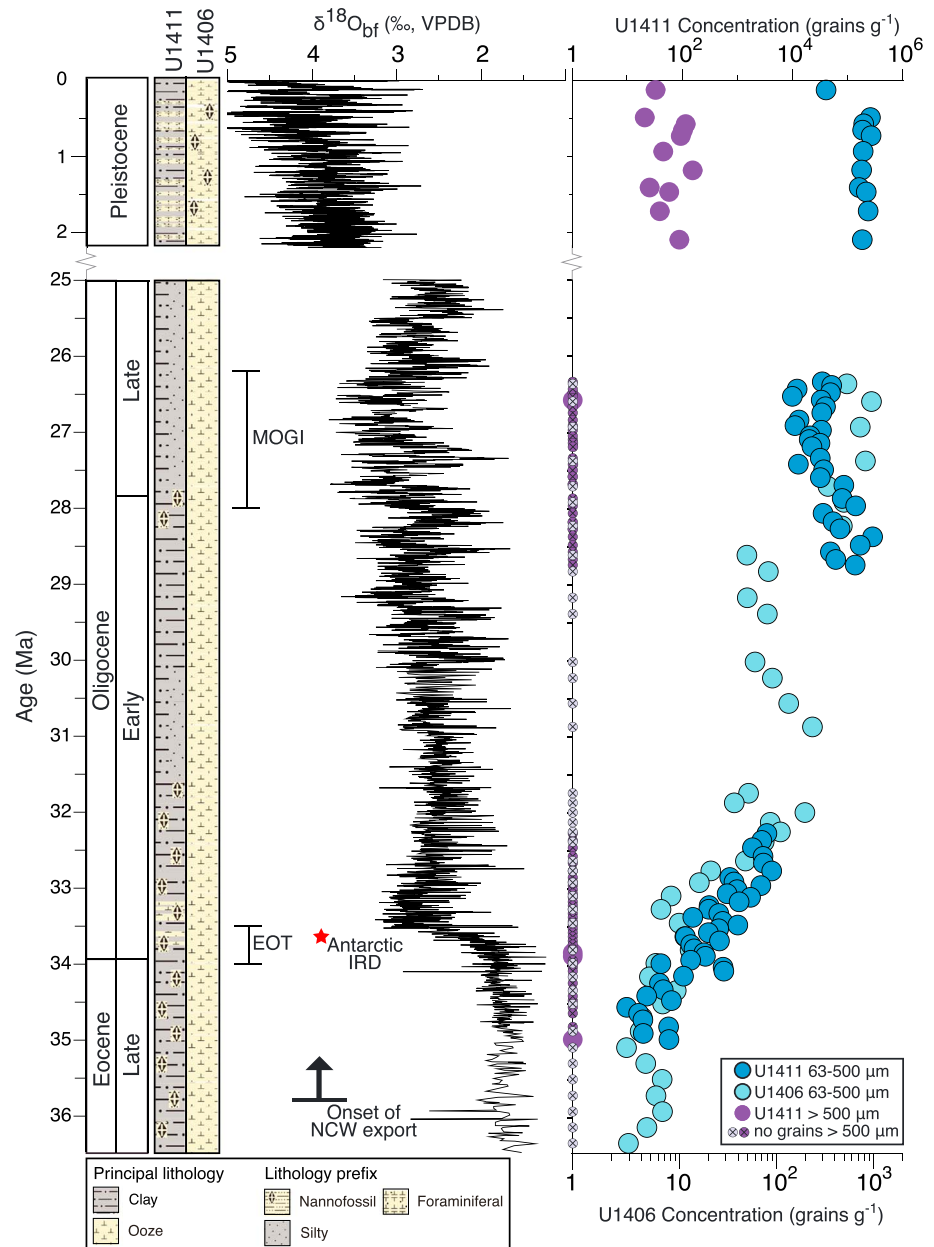
Figure 2. Temporal evolution of detrital sand grain deposition at sites U1411 and U1406 (note differing *x* axis scales). The small circles along the central *y* axis denote where samples were examined for grains >500 μm, but none were found; grains were found in the 63- to 500-μm fraction in all samples. A composite deep-water benthic foraminiferal oxygen isotope record (Liebrand et al., 2017; Zachos et al., 2001) is shown for reference. MOGI= Mid-Oligocene Glacial Interval, NCW= Northern Component Water. The red star indicates when ice-rafted debris was deposited in marginal marine Antarctic sediments (Scher et al., 2011).

superficially similar to the aggregates that we document at Site U1411. At Site 913, however, their constituent grains are coarser and more heterogeneous in composition (Figure 4e). Some of the sedimentary lithic clasts from Site 913 are underlain by deformed lamina, indicative of dropstone emplacement (Eldrett et al., 2007; Figures 4e and 4f). No equivalent structures are seen in the EOT sequence at Site U1411.

In a few cases, the grain aggregates at Site U1411 show a distinctly burrow-like morphology in cross section on the split-core surface (Figure 4d). Microcomputed tomography analysis of a core sample containing elliptical- to irregular-shaped grain aggregates further reveals a spectacular three-dimensional structure of an extensive network of millimeter-scale in diameter filaments of coarse silt and fine sands (Figures 4g and

AGU
100
ADVANCING EARTH
AND SPACE SCIENCE

Paleoceanography and Paleoclimatology

10.1029/2019PA003563

Figure 3. Scanning Electron Microscope images of quartz grains from the (a) Site U1411 EOT interval, (b) Site U1411 Pleistocene interval, and (c) Site 913 EOT interval. Scale bar = 200 μm.

4h). Most of these filaments are oriented vertically to subvertically, and some can be traced to aggregates on the split-core surface. We therefore interpret the Site U1411 aggregates as cross sections of burrow fills.

Taken together, our analysis of both grain textures and the nature of the grain aggregates provides no evidence in favor of the presence of IRD within the EOT interval of Site U1411. It remains possible, however, that the sand-sized material may have been eroded by small continental ice sheets at higher latitudes and then extensively reworked, first by meltwater and then submarine currents to the Newfoundland margin, thereby overprinting evidence of ice sheet activity in the high northern latitudes. To evaluate this possibility, next we determined the provenance of the fine sands deposited at Site U1411.

3.3. Grain Provenance and Ice Rafting

The results of Pb and Nd-Sr isotopic analysis of detrital sand from the Site U1411 EOT interval were considered alongside terrane data from the major circum-North Atlantic provinces (Figure 5). The EOT feldspars analyzed from Site U1411 have Pb isotope ratio ranges of ~17.2–18.9 ($^{206}Pb/^{204}Pb$) and ~15.3–15.6 ($^{207}Pb/^{204}Pb$; Figure 5a). $\varepsilon Nd(0)$ values of the coarse detrital fraction range from ~-18.7 to -10.2, and $^{87}Sr/^{86}Sr$ ratios range from ~0.712 to 0.720 (Figure 5b). When compared to published data from circum-North Atlantic

Table 1
Abundance of Surface Textures on Quartz Grains From the Site U1411 and 913 EOT Intervals, and the Site U1411 Pleistocene Interval

Surface texture	Abundance (%)		
	Site U1411 EOT	Site 913 EOT	Site U1411 Pleistocene
Mechanical			
-Breakage blocks	38	35	23
-Conchoidal fractures	59	83	77
-Arc step-like fractures	30	37	37
-Straight step-like fractures	16	20	17
-Isolated fractures	18	36	12
-Mechanical impact pits	37	72	63
-Gouges/striations	41	59	64
-Edge abrasion	55	46	71
-Upturned plates	34	28	40
Chemical			
-Microlayering	26	3	2
-Chemical v-pits	43	32	19
-Adhering particles	38	17	12
-Silica precipitation	84	70	65
Silica Dissolution			
-Rare-Absent	7	11	13
-Present	25	34	37
-Common	45	41	38
-Pervasive	23	14	11
Relief			
-Low	42	11	14
-Medium	43	50	52
-High	15	39	34
Roundness			
-Very angular	5	6	16
-Angular	17	24	40
-Subangular	23	45	23
-Subrounded	29	17	12
-Rounded	20	7	8
-Well rounded	6	1	1

terranes, the Pb isotope ratios of Site U1411 feldspars do not overlap with Greenland provinces of Archean or Proterozoic age of southern and western Greenland (Bailey et al., 2012; White et al., 2016). Instead, they overlap in Pb-Pb space with the local North American (Appalachian and Grenville), Scandinavian, and British/Irish provinces (Figure 5a). The Site U1411 Pb isotope data for the EOT also overlap with the Greenland Caledonides (Figures 5a and S2), but a Greenland source is ruled out by the Nd-Sr data, which show that the sands from Site U1411 are sourced from North America and/or Scandinavia from Proterozoic-age Grenville and/or Sveconorwegian provinces (Figure 5b). The Site U1411 Nd-Sr data are offset from all Greenland terranes, indicating that the Newfoundland grains were not derived from the two interpreted source areas for the IRD of EOT age at Site 913: the Greenland Caledonides and East Greenland Paleogene Volcanics (Bernard et al., 2016; Eldrett et al., 2007; Tripati et al., 2008; Tripati & Darby, 2018). The Site U1411 data are, however, comparable in Nd-Sr space to late Pleistocene glaciomarine sediments from two sites (HU90-028-20 and HU90-028-10; Figure 1) in the Gulf of St. Lawrence (Farmer et al., 2003) and to non-Heinrich event glaciomarine sediments deposited on Orphan Knoll in the Northwest Atlantic at Site EW903-GGC31 from 15 to 20 ka (Downing & Hemming, 2012). Pleistocene detrital sediments at these locations originate from the Gulf of St. Lawrence (Figure 5b), further reinforcing the idea of a local Grenville source for the EOT grains from Site U1411.

The small size of the sand-sized feldspars (~63–125 μm) from the EOT interval of Site U1411 prevents Pb isotope analysis of individual grains. Yet comparison of our Site U1411 data to the Pb isotope composition of individual and composite ice-rafted feldspars deposited in the subpolar North Atlantic at Sites V28-82 and V32-14 during ice-rafting events of the Last Glacial (Gwiazda et al., 1996; ~19–26 ka, i.e., outside of
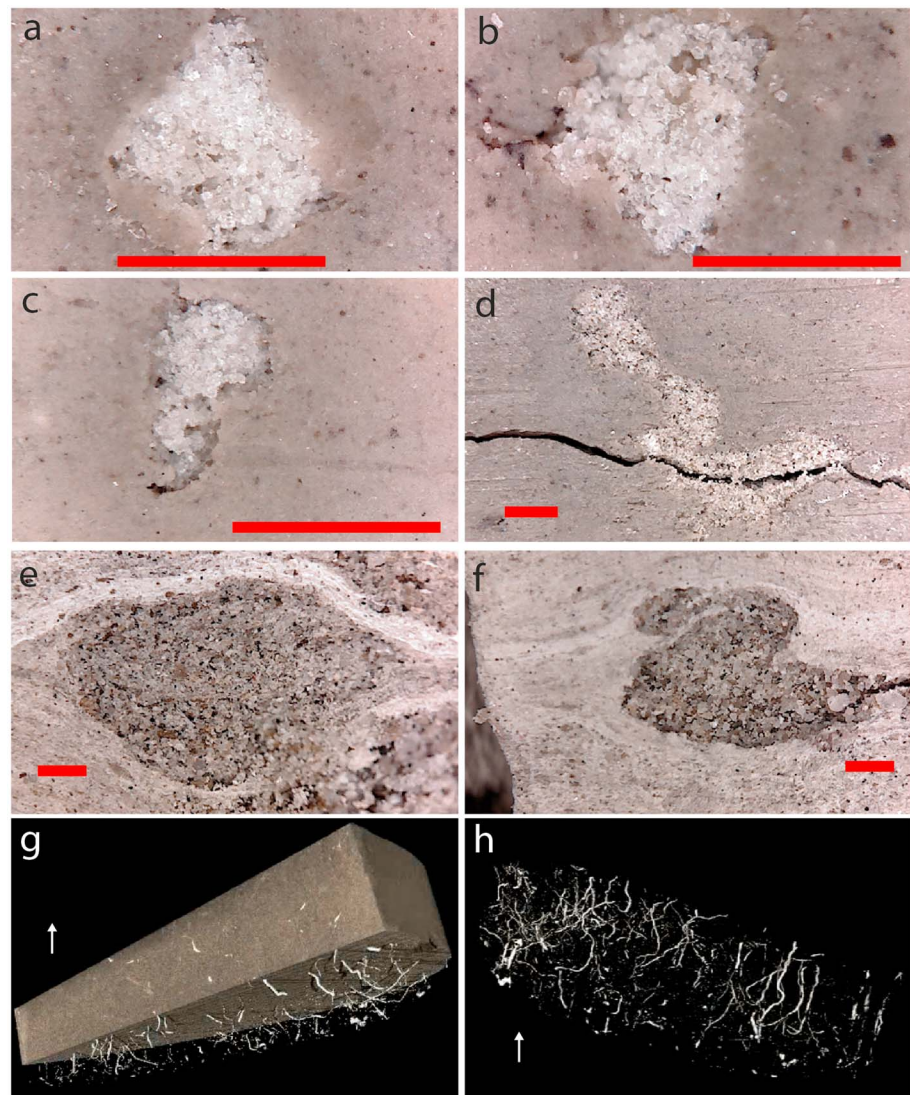
Figure 4. Grain aggregates from the Site U1411 EOT interval, (a-c) typical elliptical to irregular morphology, (d) rare elongate morphology, (e and f) Site 913 EOT interval. Scale bar = 1 mm. Computed tomography scan of Site U1411 core sample reveals that the aggregates seen at this site are cross sections of burrow-fills (g and h) Sample diameter = 10 cm; the arrow denotes stratigraphic orientation. A video file, from which (g) and (h) are captured, is available in the supporting information.

Heinrich events) illustrates that a Precambrian Greenland and/or Precambrian North American source for these grains is untenable (Figure 5a). Thus, our findings indicate that the detrital sands and silts deposited on the SENR during the EOT do not originate from Greenland or northeastern Canada. In principle, the provenance data allow for a Sveconorwegian contribution to Site U1411 sediments. Iceberg trajectory models, however, suggest that if IRD from Scandinavia were to reach the SENR, Greenland IRD would also likely reach the site, and the geochemical data presented here do not support Greenland as a source (Bigg et al., 1996, 1998, 2014). Furthermore, the grain textural analysis does not support IRD from any source. Taken together, therefore, our analyses strongly point to a local midlatitude North American-only provenance and transport by rivers and ocean currents, rather than ice rafting

4. Discussion

Our combined grain size, textural, and provenance analyses of the detrital grains deposited on the Newfoundland margin during the EOT conclusively demonstrates transport of local sediments by fluvial processes and subsequent reworking by ocean currents, rather than ice rafting. The fact that the EOT
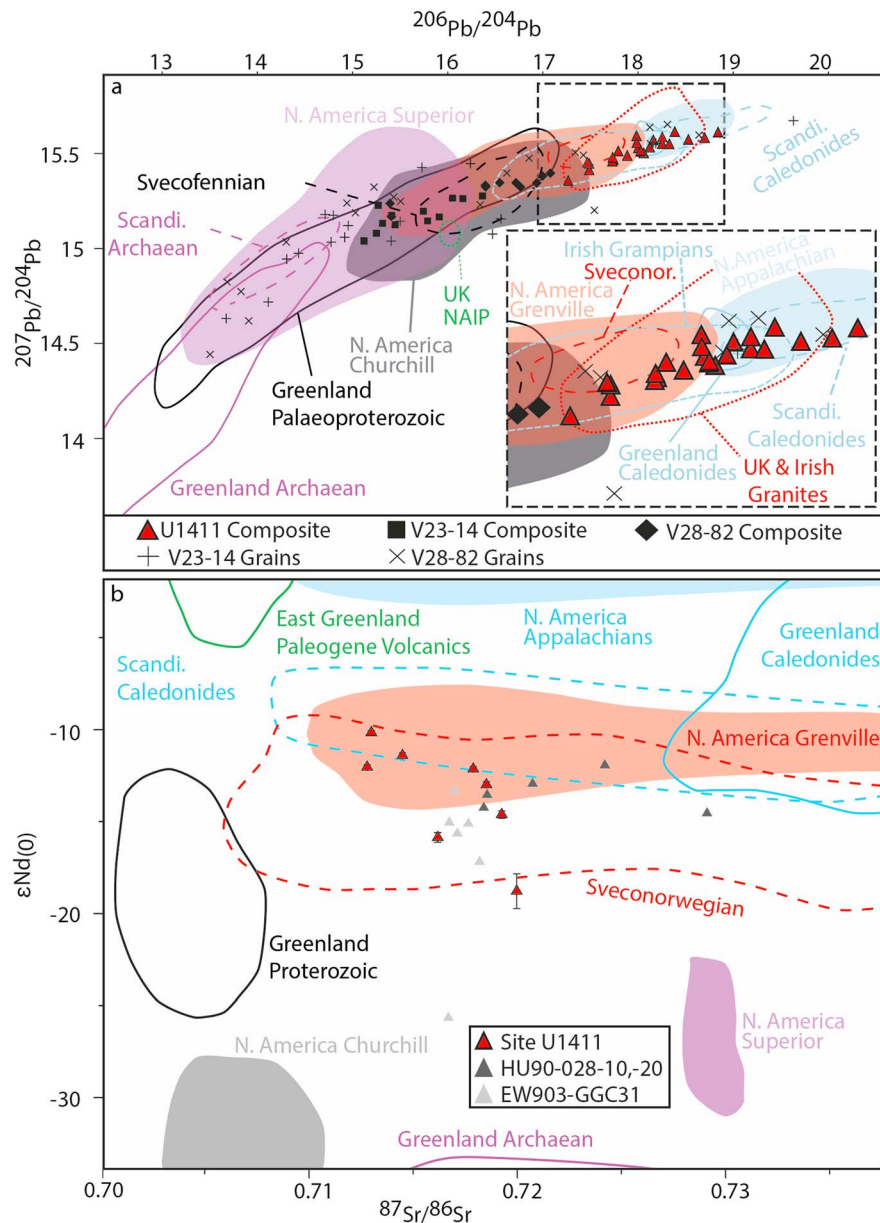
Figure 5. Radiogenic isotope provenance analysis of Eocene-Oligocene Transition-age grains from Site U1411. See Figure 1 for locations of terranes and relevant sites. (a) Pb isotopic composition of coarse feldspar composites from Site U1411, alongside data from feldspars analyzed from North Atlantic terranes and Pleistocene-age glaciomarine feldspars from Sites V23-14 and V28-8237. (b) Nd-Sr isotopic analysis of the coarse detrital fraction from Site U1411, alongside published Pb values of North Atlantic terranes and Pleistocene-age glaciomarine sediments from Sites EW903-GGC31, HU90-028-10, and HU90-028-20 (Downing & Hemming, 2012; Farmer et al., 2003). References for North Atlantic terrane data are given in Tables S2 and S3. The error is shown to two standard deviations where larger than symbol size.

intervals of the SENR have been shown not to contain IRD, contrary to the initial interpretations during shipboard work on IODP Exp. 342, argues strongly against extensive glaciation of southern and western Greenland and northeastern Canada at this time. Modeling of the formation of the Greenland Ice Sheet suggests that western Greenland only becomes glaciated once proto-ice caps that emerge in elevated regions of eastern and southern Greenland merge and spread toward Baffin Bay (Schaefer et al., 2016; Solgaard et al., 2013). The absence of any icebergs rafting from southern or western Greenland across the EOT, as shown by our findings, therefore implies that any ice cap in eastern Greenland had not expanded across the continent to the southern or western coastlines at this time.

A link to deep-water activity is further supported by the gradual increase in abundance of disseminated sand at both Sites U1406 and U1411 from the late Eocene (~35 Ma; Figure 3), at a time when the Labrador Sea is suggested (Coxall et al., 2018) to have first become a major conduit for the southward export of Northern Component Water (Figure 2). Our findings are also consistent with the suggestion that heat piracy associated with strengthened meridional overturning circulation may have helped to promote austral cooling prior to Antarctic glaciation (Coxall et al., 2018). The local provenance signal of the detrital sand on the SENR suggests that these grains were likely entrained into ocean currents locally, potentially through downslope transport from the shelf-break of the Grand Banks during the lower sea levels of the early Oligocene. The development of a higher-resolution record of grain flux at Site U1411 (and Site U1406), in combination with high-resolution benthic foraminiferal stable isotope records and a more accurate age model, will allow for further interrogation of the combination of driving forces behind the detrital sand grains.

The lack of evidence from the Newfoundland margin sites for extensive EOT glaciation in southern and western Greenland and/or northeastern Canada lends strong support to the hypothesis (DeConto et al., 2008), based on coupled climate-ice sheet model simulations, that the Cenozoic transition to a glaciated state occurred first in the Southern Hemisphere and later in the Northern Hemisphere as two different climate thresholds were crossed. This finding is consistent with the suggestion that the differing arrangement of continents at the two poles causes distinct CO_2-temperature thresholds for the establishment of major ice sheets in the two hemispheres (DeConto et al., 2008). In this interpretation, Antarctica is cold relative to the continental land masses of the Arctic because of its higher latitudinal setting, triggering extensive glaciation of Antarctica earlier than of the Arctic land masses as climate slowly deteriorated through the Cenozoic.

The lack of evidence for extensive Northern Hemisphere glaciation at the EOT is also consistent with the observed warmth of the EOT Northwest Atlantic Ocean (Liu et al., 2018), North Sea (Śliwińska et al., 2019), and on Greenland (Eldrett et al., 2009), especially in summer. Climate-forced ice sheet simulations show that the Greenland Ice Sheet of today is a relict formed under conditions colder than present (Solgaard et al., 2013). Thus, while a warm Northwest Atlantic could, in principle, prevent icebergs calved from southern and western Greenland and northeastern Canada from reaching the SENR, the warmth observed for the Northwest Atlantic Ocean would have prevented the glaciation of those areas in the first place.

The limitation of Cenozoic glaciation in the Northern Hemisphere to either an eastern Greenland ice cap, or upland outlet glaciers, also implies that there were no significant contributions to oxygen isotope-derived ice budgets from the Northern Hemisphere, with observed oxygen isotope shifts attributable to Antarctic ice volume and cooling alone (Coxall et al., 2005; Edgar et al., 2007; Lear et al., 2008).

5. Conclusions

Sediments of Eocene-to-Oligocene age from the NGS host IRD sourced from the east coast of Greenland (Eldrett et al., 2007), but we find no evidence for contemporaneous ice rafting within the North Atlantic's iceberg alley on the Newfoundland margin. This result strongly suggests that active ice calving from eastern Greenland during the EOT does not signify existence of an ice sheet large enough to extend to southern and western Greenland and that the eastern ice cap (Tripati & Darby, 2018) or outlet glaciers (Eldrett et al., 2007) that existed there at this time were not also accompanied by similar ice masses in northeastern Canada. The conspicuous detrital sands in sediments of EOT age at IODP Site U1411 were sourced locally from midlatitude terranes of North America and delivered to the Newfoundland margin by a combination of fluvial and marine processes. These findings rule out the development of large ice sheets on Greenland and in the northeastern Canadian Arctic and are consistent with EOT warmth in the Northwest Atlantic Ocean (Liu et al., 2018) and on Greenland (Eldrett et al., 2009). These results are also consistent with numerical climate-forced ice sheet simulations (Solgaard et al., 2013) that indicate that the Greenland Ice Sheet of today is a relict formed under colder conditions than present.

There is robust evidence for development of an extensive Antarctic ice sheet at the EOT (Coxall et al., 2005; Kennett, 1977; Scher et al., 2011), but our data show that large ice sheets in the Northern Hemisphere were not established at the same time. Accordingly, our data indicate the sequential rather than simultaneous development of Cenozoic ice sheets in the two hemispheres. The precise timing of the inception of major Northern Hemisphere glaciation can be tested by scientific drilling on the Newfoundland margin into sediments of Mio-Pliocene age, but our records show that the unipolar (Antarctic) icehouse state existed millions

of years before a bipolar one. The establishment of the Cenozoic unipolar (Antarctic) icehouse climate state before a bipolar one is likely attributable to the fundamental control exerted on the cryosphere by the contrasting arrangement of the polar continents, which lie at lower latitudes in the Northern Hemisphere (even more so during the EOT than today; Steinberger et al., 2015) resulting in warmer summers there than on Antarctica for a given global radiative forcing (DeConto et al., 2008).

References

Andrews, J. T., & Tedesco, K. (1992). Detrital carbonate rich sediments, North- western Labrador Sea—Implications for ice-sheet dynamics and iceberg rafting (Heinrich) events in the North-Atlantic. *Geology*, *20*, 1087–1090. https://doi.org/10.1130/0091-7613(1992)020<1087:DCRSNL>2.3.CO;2

Bailey, I., Foster, G. L., Wilson, P. A., Jovane, L., Storey, C. D., Trueman, C. N., & Becker, J. (2012). Flux and provenance of ice-rafted debris in the earliest Pleistocene sub-polar North Atlantic Ocean comparable to the last glacial maximum. *Earth and Planetary Science Letters*, *341–344*, 222–233. https://doi.org/10.1016/j.epsl.2012.05.034

Bailey, I., Hole, G. M., Foster, G. L., Wilson, P. A., Storey, C. D., Trueman, C. N., & Raymo, M. E. (2013). An alternative suggestion for the Pliocene onset of major northern hemisphere glaciation based on the geochemical provenance of North Atlantic Ocean ice-rafted debris. *Quaternary Science Reviews*, *75*, 181–194. https://doi.org/10.1016/j.quascirev.2013.06.004

Baker, J., Peate, D., Waight, T., & Meyzen, C. (2004). Pb isotopic analysis of standards and samples using a 207Pb–204Pb double spike and thallium to correct for mass bias with a double-focusing MC-ICP-MS. *Chemical Geology*, *3*(211), 275–303.

Bernard, T., Steer, P., Gallagher, K., Szulc, A., Whitham, A., & Johnson, C. (2016). Evidence for Eocene–Oligocene glaciation in the landscape of the East Greenland margin. *Geology*, *44*(11), 895–898. https://doi.org/10.1130/G38248.1

Bigg, G. R., Wadley, M. R., Stevens, D. P., & Johnson, J. A. (1996). Prediction of iceberg trajectories for the North Atlantic and Arctic oceans. *Geophysical Research Letters*, *23*(24), 3587–3590. https://doi.org/10.1029/96GL03369

Bigg, G. R., Wadley, M. R., Stevens, D. P., & Johnson, J. A. (1998). Simulations of two last glacial maximum ocean states. *Paleoceanography*, *13*(4), 340–351. https://doi.org/10.1029/98PA00402

Bigg, G. R., Wei, H. L., Wilton, D. J., Zhao, Y., Billings, S. A., Hanna, E., & Kadirkamanathan, V. (2014). A century of variation in the dependence of Greenland iceberg calving on ice sheet surface mass balance and regional climate change. *Proceedings of the Royal Society A: Mathematical, Physical and Engineering Sciences*, *470*(2166), 20,130,662–20,130,662. https://doi.org.10.1098/rspa.2013.0662

Bolton, C. T., Bailey, I., Friedrich, O., Tachikawa, K., Garidel-Thoron, T., Vidal, L., et al. (2018). North Atlantic mid-latitude surface-circulation changes through the Plio-Pleistocene intensification of northern hemisphere glaciation. *Paleoceanography*, *33*, 1186–1205. https://doi.org/10.1029/2018PA003412

Boyle, P. R., Romans, B. W., Tucholke, B. E., Norris, R. D., Swift, S. A., & Sexton, P. F. (2017). Cenozoic North Atlantic deep circulation history recorded in contourite drifts, offshore Newfoundland, Canada. *Marine Geology*, *385*(Supplement C), 185–203. https://doi.org/10.1016/j.margeo.2016.12.014

Coxall, H. K., Huck, C. E., Huber, M., Lear, C. H., Legarda-Lisarri, A., O'Regan, M., et al. (2018). Export of nutrient rich Northern Component Water preceded early Oligocene Antarctic glaciation. *Nature Geoscience*, *11*(3), 190. https://doi.org/10.1038/s41561-018-0069-9

Coxall, H. K., Wilson, P. A., Pälike, H., Lear, C. H., & Backman, J. (2005). Rapid stepwise onset of Antarctic glaciation and deeper calcite compensation in the Pacific Ocean. *Nature*, *433*(7021), 53–57. https://doi.org/10.1038/nature03135

Davies, A., Kemp, A. E. S., & Pike, J. (2009). Late Cretaceous seasonal ocean variability from the Arctic. *Nature*, *460*, 254–258. https://doi:10.1038/nature08141

Dawber, C. F., & Tripati, A. K. (2011). Constraints on glaciation in the middle Eocene (46–37 Ma) from Ocean Drilling Program (ODP) Site 1209 in the tropical Pacific Ocean. *Paleoceanography*, *26*, PA2208. https://doi.org/10.1029/2010PA002037

DeConto, R. M., Pollard, D., Wilson, P. A., Pälike, H., Lear, C. H., & Pagani, M. (2008). Thresholds for Cenozoic bipolar glaciation. *Nature*, *455*(7213), 652–656. https://doi.org/10.1038/nature07337

Downing, G. E., & Hemming, S. R. (2012). Late glacial and deglacial history of ice rafting in the Labrador Sea: A perspective from radiogenic isotopes in marine sediments. *Special Paper of the Geological Society of America*, *487*, 113–124. https://doi.org/10.1130/2012.2487(07)

Dunhill, G. (1998). Comparison of sea-ice rafted debris; : grain Grain size, surface features, and grain shape. (USGS Numbered Series No. 98–367) (pp. 98–367). U.S. Geological Survey. Retrieved from http://pubs.er.usgs.gov/publication/ofr98367

Edgar, K. M., Wilson, P. A., Sexton, P. F., & Suganuma, Y. (2007). No extreme bipolar glaciation during the main Eocene calcite compensation shift. *Nature*, *448*(7156), 908–911. https://doi.org/10.1038/nature06053

Eldrett, J. S., Greenwood, D. R., Harding, I. C., & Huber, M. (2009). Increased seasonality through the Eocene to Oligocene transition in northern high latitudes. *Nature*, *459*(7249), 969–973. https://doi.org/10.1038/nature08069

Eldrett, J. S., Harding, I. C., Wilson, P. A., Butler, E., & Roberts, A. P. (2007). Continental ice in Greenland during the Eocene and Oligocene. *Nature*, *446*(7132), 176–179. https://doi.org/10.1038/nature05591

Farmer, G. L., Barber, D., & Andrews, J. (2003). Provenance of Late Quaternary ice-proximal sediments in the North Atlantic: Nd, Sr and Pb isotopic evidence. *Earth and Planetary Science Letters*, *209*(1–2), 227–243. https://doi.org/10.1016/S0012-821X(03)00068-2

Garzanti, E., Ando, S., & Vezzoli, G. (2008). Settling equivalence of detrital minerals and grain-size dependence of sediment composition. *Earth and Planetary Science Letters*, *273*(1-2), 138–151. https://doi.org/10.1016/j.epsl.2008.06.020

Gwiazda, R. H., Hemming, S. R., & Broecker, W. S. (1996). Tracking the sources of icebergs with lead isotopes: The provenance of ice-rafted debris in Heinrich layer 2. *Paleoceanography*, *11*(1), 77–93. https://doi.org/10.1029/95PA03135

Hambrey, M. J., & Barrett, P. J. (1993). Cenozoic sedimentary and climatic record, Ross Sea region, Antarctica. *The Antarctic Paleoenvironment: A Perspective on Global Change: Part Two*, 91–124. https://doi.org/10.1029/AR060p0091

Helland, P. E., & Holmes, M. A. (1997). Surface textural analysis of quartz sand grains from ODP Site 918 off the southeast coast of Greenland suggests glaciation of southern Greenland at 11 Ma. *Palaeogeography, Palaeoclimatology, Palaeoecology*, *135*(1–4), 109–121. https://doi.org/10.1016/S0031-0182(97)00025-4

Kennett, J. P. (1977). Cenozoic evolution of Antarctic glaciation, the circum-Antarctic Ocean, and their impact on global paleoceanography. *Journal of Geophysical Research*, *82*(27), 3843–3860. https://doi.org/10.1029/JC082i027p03843

Krinsley, D. H., & Doornkamp, J. C. (2011). *Atlas of Quartz Sand Surface Textures*. Cambridge: Cambridge University Press.

Lang, D. C., Bailey, I., Wilson, P. A., Beer, C. J., Bolton, C. T., Friedrich, O., et al. (2014). The transition on North America from the warm humid Pliocene to the glaciated Quaternary traced by eolian dust deposition at a benchmark North Atlantic Ocean drill site. *Quaternary Science Reviews*, *93*, 125–141. https://doi.org/10.1016/j.quascirev.2014.04.005

Larsen, H. C., Saunders, A. D., Clift, P. D., Beget, J., Wei, W., & Spezzaferri, S. (1994). Seven Million Years of Glaciation in Greenland. *Science*, *264*(5161), 952–955. https://doi.org/10.2307/2883753

Lear, C. H., Bailey, T. R., Pearson, P. N., Coxall, H. K., & Rosenthal, Y. (2008). Cooling and ice growth across the Eocene-Oligocene Transition. *Geology*, *36*(3), 251–254. https://doi.org/10.1130/G24584A.1

Liebrand, D., Bakker, A. T. M. de, Beddow, H. M., Wilson, P. A., Bohaty, S. M., Ruessink, G., et al. (2017). Evolution of the early Antarctic ice ages. *Proceedings of the National Academy of Sciences of the United States of America*, *114* (15) 3867-3872. https://doi.org/10.1073/pnas.1615440114

Liu, Z., He, Y., Jiang, Y., Wang, H., Liu, W., Bohaty, S. M., & Wilson, P. A. (2018). Transient temperature asymmetry between hemispheres in the Palaeogene Atlantic Ocean. *Nature Geoscience*. https://doi.org/10.1038/s41561-018-0182-9

Mahaney, W. C., Stewart, A., & Kalm, V. (2001). Quantification of SEM microtextures useful in sedimentary environmental discrimination. *Boreas*, *30*(2), 165–171. https://doi.org/10.1111/j.1502-3885.2001.tb01220.x

Miller, K. G., & Tucholke, B. E. (1983). Development of Cenozoic abyssal circulation south of the Greenland-Scotland Ridge. In *Structure and Development of the Greenland-Scotland Ridge* (pp. 549–589). New York: Springer. https://doi.org/10.1007/978-1-4613-3485-9_27

Miller, K. G., Wright, J. D., & Fairbanks, R. G. (1991). Unlocking the Ice House: Oligocene-Miocene oxygen isotopes, eustasy, and margin erosion. *Journal of Geophysical Research*, *96*(B4), 6829–6848. https://doi.org/10.1029/90JB02015

Moran, K., Backman, J., Brinkhuis, H., Clemens, S. C., Cronin, T., Dickens, G. R., et al. (2006). The Cenozoic palaeoenvironment of the Arctic Ocean. *Nature*, *441*(7093), 601–605. https://doi.org/10.1038/nature04800

Norris, R. D., Wilson, P. A., Blum, P., & the Expedition 342 Scientists. (2014). Proceedings IODP Leg 342. Retrieved from iodp.org/proceedings/342/iodp.htm

Powers, M. C. (1953). A New new Roundness roundness Scale scale for Sedimentary sedimentary Particlesparticles. *Journal of Sedimentary Research*, *23*(2), 117–119. https://doi.org/10.1306/D4269567-2B26-11D7-8648000102C1865D

Raymo, M. E., Ruddiman, W. F., Backman, J., Clement, B. M., & Martinson, D. G. (1989). Late Pliocene variation in northern hemisphere ice sheets and North Atlantic deep water circulation. *Paleoceanography*, *4*(4), 413–446. https://doi.org.10.1029/pa004i004p00413

Schaefer, J. M., Finkel, R. C., Balco, G., Alley, R. B., Caffee, M. W., Briner, J. P., et al. (2016). Greenland was nearly ice-free for extended periods during the Pleistocene. *Nature*, *540*(7632), 252–255. https://doi.org/10.1038/nature20146

Scher, H. D., Bohaty, S. M., Zachos, J. C., & Delaney, M. L. (2011). Two-stepping into the icehouse: East Antarctic weathering during progressive ice-sheet expansion at the Eocene–Oligocene transition. *Geology*, *39*(4), 383–386. https://doi.org/10.1130/G31726.1

Shackleton, N. J., Backman, J., Zimmerman, H., Kent, D. V., Hall, M. A., Roberts, D. G., et al. (1984). Oxygen isotope calibration of the onset of ice-rafting and history of glaciation in the North Atlantic region. *Nature*, *307*(5952), 620–623. https://doi.org/10.1038/307620a0

Śliwińska, K. K., Thomsen, E., Schouten, S., Schoon, P. L., & Heilmann-Clausen, C. (2019). Climate-and gateway-driven cooling of Late Eocene to earliest Oligocene sea surface temperatures in the North Sea Basin. *Scientific Reports*, *9*(1), 4458. https://doi.org/10.1038/s41598-019-41013-7

Solgaard, A. M., Bonow, J. M., Langen, P. L., Japsen, P., & Hvidberg, C. S. (2013). Mountain building and the initiation of the Greenland Ice Sheet. *Palaeogeography, Palaeoclimatology, Palaeoecology*, *392*, 161–176. https://doi.org/10.1016/j.palaeo.2013.09.019

St. John, K. (2008). Cenozoic ice-rafting history of the central Arctic Ocean: Terrigenous sands on the Lomonosov Ridge. *Paleoceanography*, *23*, PA1S05. https://doi.org/10.1029/2007PA001483

St. John, K., Passchier, S., Tantillo, B., Darby, D., & Kearns, L. E. (2015). Microfeatures of modern sea-ice-rafted sediment and implications for paleo-sea-ice reconstructions. *Annals of Glaciology*, *56*(69), 89–93. https://doi.org/10.3189/2015AoG69A586

Steinberger, B., Spakman, W., Japsen, P., & Torsvik, T. H. (2015). The key role of global solid-Earth processes in preconditioning Greenland's glaciation since the Pliocene. *Terra Nova*, *27*(1), 1–8. https://doi.org/10.1111/ter.12133

Tripati, A., Backman, J., Elderfield, H., & Ferretti, P. (2005). Eocene bipolar glaciation associated with global carbon cycle changes. *Nature*, *436*(7049), 341–346. https://doi.org/10.1038/nature03874

Tripati, A., & Darby, D. (2018). Evidence for ephemeral middle Eocene to early Oligocene Greenland glacial ice and pan-Arctic sea ice. *Nature Communications*, *9*(1), 1038. https://doi.org/10.1038/s41467-018-03180-5

Tripati, A. K., Eagle, R. A., Morton, A., Dowdeswell, J. A., Atkinson, K. L., Bahé, Y., et al. (2008). Evidence for glaciation in the Northern Hemisphere back to 44 Ma from ice-rafted debris in the Greenland Sea. *Earth and Planetary Science Letters*, *265*(1–2), 112–122. https://doi.org/10.1016/j.epsl.2007.09.045

White, L. F., Bailey, I., Foster, G. L., Allen, G., Kelley, S. P., Andrews, J. T., et al. (2016). Tracking the provenance of Greenland-sourced, Holocene aged, individual sand-sized ice-rafted debris using the Pb-isotope compositions of feldspars and 40Ar/39Ar ages of hornblendes. *Earth and Planetary Science Letters*, *433*, 192–203. https://doi.org/10.1016/j.epsl.2015.10.054

Williams, A. T., & Morgan, P. (1993). Scanning electron microscope evidence for offshore-onshore sand transport at Fire Island, New York, USA. *Sedimentology*, *40*(1), 63–77. https://doi.org/10.1111/j.1365-3091.1993.tb01091.x

Zachos, J. C., Pagani, M., Sloan, L., Thomas, E., & Billups, K. (2001). Trends, Rhythms, and Aberrations in Global Climate 65 Ma to Present. *Science*, *292*(5517), 686–693. https://doi.org/10.1126/science.1059412

Zachos, J. C., Quinn, T. M., & Salamy, K. A. (1996). High-resolution (104 years) deep-sea foraminiferal stable isotope records of the Eocene-Oligocene climate transition. *Paleoceanography*, *11*(3), 251–266. https://doi.org/10.1029/96PA00571

References From the Supporting Information

Aleinikoff, J. N., Walter, M., Kunk, M. J., & Hearn, P. P. (1993). Do ages of authigenic K-feldspar date the formation of Mississippi Valley-type Pb-Zn deposits, central and southeastern United States?: Pb isotopic evidence. *Geology*, *21*(1), 73–76. https://doi.org/10.1130/0091-7613(1993)021<0073:DAOAKF>2.3.CO;2

Andersen, T., Andresen, A., & Sylvester, A. G. (2001). Nature and distribution of deep crustal reservoirs in the southwestern part of the Baltic Shield: Evidence from Nd, Sr and Pb isotope data on late Sveconorwegian granites. *Journal of the Geological Society*, *158*(2), 253–267. https://doi.org/10.1144/jgs.158.2.253

Andersson, U. B., Neymark, L. A., & Billström, K. (2001). Petrogenesis of Mesoproterozoic (Subjotnian) rapakivi complexes of central Sweden: Implications from U–Pb zircon ages, Nd, Sr and Pb isotopes. *Earth and Environmental Science Transactions of the Royal Society of Edinburgh*, *92*(3), 201–228. https://doi.org/10.1017/S0263593300000237

Andreasen, R., Peate, D. W., & Brooks, C. K. (2004). Magma plumbing systems in large igneous provinces: Inferences from cyclical variations in Palaeogene East Greenland basalts. *Contributions to Mineralogy and Petrology*, *147*(4), 438–452. https://doi.org/10.1007/s00410-004-0566-2

Ashwal, L. D., Wooden, J. L., & Emslie, R. F. (1986). Sr, Nd and Pb isotopes in Proterozoic intrusives astride the Grenville Front in Labrador: Implications for crustal contamination and basement mapping. *Geochimica et Cosmochimica Acta*, *50*(12), 2571–2585. https://doi.org/10.1016/0016-7037(86)90211-5

Ashwal, L. D., & Wooden, J. L. (1989). River Valley pluton, Ontario: A late-Archean/early-Proterozoic anorthositic intrusion in the Grenville Province. *Geochimica et Cosmochimica Acta*, *53*(3), 633–641. https://doi.org/10.1016/0016-7037(89)90006-9

Ayuso, R. A., & Bevier, M. L. (1991). Regional differences in PB isotopic compositions of feldspars in plutonic rocks of the northern Appalachian Mountains, U.S.A., and Canada: A geochemical method of terrane correlation. *Tectonics*, *10*(1), 191–212. https://doi.org/10.1029/90TC02132

Baadsgaard, H., Nurman, A. P., Rosing, M., Bridgwater, D., & Longstaffe, F. J. (1986). Alteration and metamorphism of Amitsoq gneisses from the Isukasia area, West Greenland: Recommendations for isotope studies of the early crust. *Geochimica et Cosmochimica Acta*, *50*(10), 2165–2172. https://doi.org/10.1016/0016-7037(86)90071-2

Baadsgaard, H., Nutman, A. P., & Bridgwater, D. (1986). Geochronology and isotopic variation of the early Archaean Amitsoq gneisses of the Isukasia area, southern West Greenland. *Geochimica et Cosmochimica Acta*, *50*(10), 2173–2183. https://doi.org/10.1016/0016-7037(86)90072-4

Barling, J., Weis, D., & Demaiffe, D. (2000). A Sr-, Nd-and Pb-isotopic investigation of the transition between two megacyclic units of the Bjerkreim–Sokndal layered intrusion, south Norway. *Chemical Geology*, *165*(1), 47–65. https://doi.org/10.1016/S0009-2541(99)00163-1

Bernstein, S., Kelemen, P. B., Tegner, C., Kurz, M. D., Blusztajn, J., & Brooks, C. K. (1998). Post-breakup basaltic magmatism along the East Greenland Tertiary rifted margin. *Earth and Planetary Science Letters*, *160*(3–4), 845–862. https://doi.org/10.1016/S0012-821X(98)00132-0

Birkeland, A., Ihlen, P. M., & Bjorlykke, A. (1993). The sources of metals in sulfide deposits in the Helgeland nappe complex, north-central Norway; Pb isotope evidence. *Economic Geology*, *88*(7), 1810–1829. https://doi.org/10.2113/gsecongeo.88.7.1810

Birkeland, A., Nordgulen, Ø., Cumming, G. L., & Bjørlykke, A. (1993). Pb-Nd-Sr isotopic constraints on the origin of the Caledonian Bindal Batholith, central Norway. *Lithos*, *29*(3-4), 257–271. https://doi.org/10.1016/0024-4937(93)90020-D

Blaxland, A. B., Aftalion, M., & van Breemen, O. (1979). Pb isotopic composition of feldspars from Scottish Caledonian granites, and the nature of the underlying crust. *Scottish Journal of Geology*, *15*(2), 139–151. https://doi.org/10.1144/sjg15020139

Brown, P. E., Dempster, T. J., Hutton, D. H. W., & Becker, S. M. (2003). Extensional tectonics and mafic plutons in the Ketilidian rapakivi granite suite of South Greenland. *Lithos*, *67*(1), 1–13. https://doi.org/10.1016/S0024-4937(02)00212-8

Carignan, J., Gariépy, C., Machado, N., & Rive, M. (1993). Pb isotopic geochemistry of granitoids and gneisses from the late Archean Pontiac and Abitibi Subprovinces of Canada. *Chemical Geology*, *106*(3), 299–315. https://doi.org/10.1016/0009-2541(93)90033-F

Connelly, J. N., & Thrane, K. (2005). Rapid determination of Pb isotopes to define Precambrian allochthonous domains: An example from West Greenland. *Geology*, *33*(12), 953–956. https://doi.org/10.1130/G21720.1

Cosca, M. A., Mezger, K., & Essene, E. J. (1998). The Baltica-Laurentia connection: Sveconorwegian (Grenvillian) metamorphism, cooling, and unroofing in the Bamble sector, Norway. *The Journal of Geology*, *106*(5), 539–552. https://doi.org/10.1086/516040

DeWolf, C. P., & Mezger, K. (1994). Lead isotope analyses of leached feldspars: Constraints on the early crustal history of the Grenville Orogen. *Geochimica et Cosmochimica Acta*, *58*(24), 5537–5550. https://doi.org/10.1016/0016-7037(94)90248-8

Dickin, A. P., & Jones, N. W. (1983). Isotopic evidence for the age and origin of pitchstones and felsites, Isle of Eigg, NW Scotland. *Journal of the Geological Society*, *140*(4), 691–700. https://doi.org/10.1144/gsjgs.140.4.0691

Doe, B. R. (1976). Lead isotope data bank; 2,624 samples and analyses cited. (USGS Numbered Series No. 76–201). U.S. Geological Survey. Retrieved from http://pubs.er.usgs.gov/publication/ofr76201

Gariépy, C., & Allègre, C. J. (1985). The lead isotope geochemistry and geochronology of late-kinematic intrusives from the Abitibi greenstone belt, and the implications for late Archaean crustal evolution. *Geochimica et Cosmochimica Acta*, *49*(11), 2371–2383. https://doi.org/10.1016/0016-7037(85)90237-6

Gariépy, C., Verner, D., & Doig, R. (1990). Dating Archean metamorphic minerals southeast of the Grenville front, western Quebec, using Pb isotopes. *Geology*, *18*(11), 1078–1081. https://doi.org/10.1130/0091-7613(1990)018<1078:DAMMSO>2.3.CO;2

Halla, J., & Heilimo, E. (2009). Deformation-induced Pb isotope exchange between K-feldspar and whole rock in Neoarchean granitoids: Implications for assessing Proterozoic imprints. *Chemical Geology*, *265*(3–4), 303–312. https://doi.org/10.1016/j.chemgeo.2009.04.007

Hansen, B. T., & Friderichsen, J. D. (1989). The influence of recent lead loss on the interpretation of disturbed U-Pb systems in zircons from igneous rocks in East Greenland. *Lithos*, *23*(3), 209–223. https://doi.org/10.1016/0024-4937(89)90006-6

Hansen, H., & Nielsen, T. F. D. (1999). Crustal contamination in Palaeogene East Greenland flood basalts: plumbing Plumbing system evolution during continental rifting. *Chemical Geology*, *157*(1–2), 89–118. https://doi.org/10.1016/S0009-2541(98)00196-X

Henry, P., Stevenson, R. K., & Gariépy, C. (1998). Late Archean Mantle Composition and Crustal Growth in the Western Superior Province of Canada: Neodymium and Lead Isotopic Evidence from the Wawa, Quetico, and Wabigoon Subprovinces. *Geochimica et Cosmochimica Acta*, *62*(1), 143–157. https://doi.org/10.1016/S0016-7037(97)00324-4

Hinchey, J. G., & Hattori, K. H. (2007). Lead isotope study of the late Archean Lac des Iles palladium deposit, Canada: enrichment Enrichment of platinum group elements by ponded sulfide melt. *Mineralium Deposita*, *42*(6), 601–611. https://doi.org/10.1007/s00126-007-0129-3

Immonen, N. (2013). Surface microtextures of ice-rafted quartz grains revealing glacial ice in the Cenozoic Arctic. *Palaeogeography, Palaeoclimatology, Palaeoecology*, *374*, 293–302. https://doi.org/10.1016/j.palaeo.2013.02.003

Jacobsen, S. B., & Dymek, R. F. (1988). Nd and Sr isotope systematics of clastic metasediments from Isua, West Greenland: Identification of pre-3.8 Ga Differentiated Crustal Components. *Journal of Geophysical Research*, *93*(B1), 338–354. https://doi.org/10.1029/JB093iB01p00338

Kalsbeek, F., Pidgeon, R. T., & Taylor, P. N. (1987). Nagssugtoqidian mobile belt of West Greenland: a cryptic 1850 Ma suture between two Archaean continents—chemical Chemical and isotopic evidence. *Earth and Planetary Science Letters*, *85*(4), 365–385. https://doi.org/10.1016/0012-821X(87)90134-8

Kalsbeek, F., & Taylor, P. N. (1985). Isotopic and chemical variation in granites across a Proterozoic continental margin—the The Ketilidian mobile belt of South Greenland. *Earth and Planetary Science Letters*, *73*(1), 65–80. https://doi.org/10.1016/0012-821X(85)90035-4

Kamber, B. S., Collerson, K. D., Moorbath, S., & Whitehouse, M. J. (2003). Inheritance of early Archaean Pb-isotope variability from long-lived Hadean protocrust. *Contributions to Mineralogy and Petrology*, *145*(1), 25–46. https://doi.org/10.1007/s00410-002-0429-7

LeHuray, A. P. (1986). Isotopic evidence for a tectonic boundary between the Kings Mountain and Inner Piedmont belts, southern Appalachians. *Geology*, *14*(9), 784–787. https://doi.org/10.1130/0091-7613(1986)14<784:IEFATB>2.0.CO;2

Liu, H.-C., You, C.-F., Huang, K.-F., & Chung, C.-H. (2012). Precise determination of triple Sr isotopes (δ^{87}Sr and δ^{88}Sr) using MC-ICP-MS. *Talanta*, *88*, 338–344. https://doi.org/10.1016/j.talanta.2011.10.050

Marcantonio, F., McNutt, R. H., Dickin, A. P., & Heaman, L. M. (1990). Isotopic evidence for the crustal evolution of the Frontenac Arch in the Grenville Province of Ontario, Canada. *Chemical Geology*, *83*(3), 297–314. https://doi.org/10.1016/0009-2541(90)90286-G

McCulloch, M. T., & Wasserburg, G. J. (1978). Sm-Nd and Rb-Sr Chronology chronology of Continental continental Crust crust Formationformation. *Science*, *200*(4345), 1003–1011. https://doi.org/10.1126/science.200.4345.1003

Morton, A. C., & Parson, L. M. (1988). *Early Tertiary Volcanism and the Opening of the NE Atlantic*. Oxford: Blackwell Scientific Publications.

Ripley, E. M., Lambert, D. D., & Frick, L. R. (1998). Re-Os, Sm-Nd, and Pb isotopic constraints on mantle and crustal contributions to magmatic sulfide mineralization in the Duluth Complex. *Geochimica et Cosmochimica Acta*, *62*(19–20), 3349–3365. https://doi.org/10.1016/S0016-7037(98)00235-X

Robertson, S. (1986). Evolution of the late Archaean lower continental crust in southern West Greenland. *Geological Society, London, Special Publications*, *24*(1), 251–260. https://doi.org/10.1144/GSL.SP.1986.024.01.22

Saunders, A. D., Kempton, P. D., Fitton, J. G., & Larsen, L. M. (1999). Sr, Nd, and Pb isotopes and trace element geochemistry of basalts from the Southeast Greenland margin. In *Proceedings of the Ocean Drilling Program. Scientific results* (Vol. 163, pp. 77–93). College Station, TX: Ocean Drilling Program. Retrieved from. http://cat.inist.fr/?aModele=afficheN&cpsidt=1097797

Shennan, S. (1988). *Quantifying Archaeology*. Edinburgh: Edinburgh University Press Academic Press. Retrieved from. http://trove.nla.gov.au/version/14995881

Sinha, A. K. (1970). Model lead and radiometric ages from the Churchill Province, Canadian Shield. *Geochimica et Cosmochimica Acta*, *34*(10), 1089–1106. https://doi.org/10.1016/0016-7037(70)90164-X

Stendal, H., & Frei, R. (2008). Mineral occurrences in central East Greenland (70°N-75°N) and their relation to the Caledonian orogeny- A Sr-Nd-Pb isotopic study of scheelite. *Memoir - Geological Society of America*, *202*, 293–306. https://doi.org/10.1130/2008.1202(12)

Stevenson, R., Henry, P., & Gariépy, C. (1999). Assimilation–fractional crystallization origin of Archean Sanukitoid Suites: Western Superior Province, Canada. *Precambrian Research*, *96*(1–2), 83–99. https://doi.org/10.1016/S0301-9268(99)00009-1

Tanaka, T., Togashi, S., Kamioka, H., Amakawa, H., Kagami, H., Hamamoto, T., et al. (2000). JNdi-1: A neodymium isotopic reference in consistency with LaJolla neodymium. *Chemical Geology*, *168*(3–4), 279–281. https://doi.org/10.1016/S0009-2541(00)00198-4

Taylor, R. N., Ishizuka, O., Michalik, A., Milton, J. A., & Croudace, I. W. (2015). Evaluating the precision of Pb isotope measurement by mass spectrometry. *Journal of Analytical Atomic Spectrometry*, *30*(1), 198–213. https://doi.org/10.1039/C4JA00279B

Tilton, G. R., & Kwon, S.-T. (1990). Isotopic evidence for crust-mantle evolution with emphasis on the Canadian Shield. *Chemical Geology*, *83*(3), 149–163. https://doi.org/10.1016/0009-2541(90)90277-E

Tilton, G. R., & Steiger, R. H. (1969). Mineral ages and isotopic composition of primary lead at Manitouwadge, Ontario. *Journal of Geophysical Research*, *74*(8), 2118–2132. https://doi.org/10.1029/JB074i008p02118

Tomascak, P. B., Krogstad, E. J., & Walker, R. J. (1996). Nature of the crust in Maine, USA: evidence from the Sebago batholith. *Contributions to Mineralogy and Petrology*, *125*(1), 45–59. https://doi.org/10.1007/s004100050205

Tyrrell, S., Haughton, P. D. W., Daly, J. S., Kokfelt, T. F., & Gagnevin, D. (2006). The use of the common Pb isotope composition of detrital K-feldspar grains as a provenance tool and its application to Upper Carboniferous paleodrainage, northern England. *Journal of Sedimentary Research*, *76*(2), 324–345. https://doi.org/10.2110/jsr.2006.023

Tyrrell, S., Haughton, P. D., & Daly, J. S. (2007). Drainage reorganization during breakup of Pangea revealed by in-situ Pb isotopic analysis of detrital K-feldspar. *Geology*, *35*(11), 971–974. https://doi.org/10.1130/G4123A.1

Vidal, P., Blais, S., Jahn, B. M., Capdevila, R., & Tilton, G. R. (1980). U-Pb and Rb-Sr systematics of the Suomussalmi Archean greenstone belt (eastern Finland). *Geochimica et Cosmochimica Acta*, *44*(12), 2033–2044. https://doi.org/10.1016/0016-7037(80)90201-X

Vitrac, A. M., Albarede, F., & Allègre, C. J. (1981). Lead isotopic composition of Hercynian granitic K-feldspars constrains continental genesis. *Nature*, *291*(5815), 460–464. https://doi.org/10.1038/291460a0

Weis, D. (1986). Genetic implications of Pb isotopic geochemistry in the Rogaland anorthositic complex (southwest Norway). *Chemical Geology*, *57*(1), 181–199. https://doi.org/10.1016/0009-2541(86)90102-6

Whalen, J. B., Jenner, G. A., Longstaffe, F. J., Robert, F., & Gariépy, C. (1996). Geochemical and Isotopic (O, Nd, Pb and Sr) Constraints on A-type Granite Petrogenesis Based on the Topsails Igneous Suite, Newfoundland Appalachians. *Journal of Petrology*, *37*(6), 1463–1489. https://doi.org/10.1093/petrology/37.6.1463

Zartman, R. E., & Wasserburg, G. J. (1969). The isotopic composition of lead in potassium feldspars from some 1.0-b.y. old North American igneous rocks. *Geochimica et Cosmochimica Acta*, *33*(8), 901–942. https://doi.org/10.1016/0016-7037(69)90104-5